HHS Public Access

Author manuscript

Stroke. Author manuscript; available in PMC 2016 April 14.

Published in final edited form as:

Stroke. 2010 September ; 41(9): 2064–2070. doi:10.1161/STROKEAHA.109.575993.

Biodistribution of Neural Stem Cells After Intravascular Therapy for Hypoxic–Ischemia

Arjun V. Pendharkar, BS, **Josh Y. Chua, BS**, **Robert H. Andres, MD**, **Nancy Wang**, **Xavier Gaeta, BS**, **Hui Wang, PhD**, **Abhijit De, PhD**, **Raymond Choi, MD**, **Shawn Chen, PhD**, **Brian K. Rutt, PhD**, **Sanjiv S. Gambhir, MD, PhD**, and **Raphael Guzman, MD**

Department of Neurosurgery (A.V.P., J.Y.C., R.H.A., N.W., X.G., R.C., R.G.), Stanford University School of Medicine, Stanford, Calif; the Molecular Imaging Program at Stanford (MIPS; H.W., A.D., S.C., B.K.R., S.S.G.), Stanford University School of Medicine, Stanford, Calif; and the Department of Radiology (S.C., B.K.R., S.S.G.), Stanford University School of Medicine, Stanford, Calif.

Abstract

Background and Purpose—Intravascular transplantation of neural stem cells represents a minimally invasive therapeutic approach for the treatment of central nervous system diseases. The cellular biodistribution after intravascular injection needs to be analyzed to determine the ideal delivery modality. We studied the biodistribution and efficiency of targeted central nervous system delivery comparing intravenous and intra-arterial (IA) administration of neural stem cells after brain ischemia.

Methods—Mouse neural stem cells were transduced with a firefly luciferase reporter gene for bioluminescence imaging (BLI). Hypoxic–ischemia was induced in adult mice and reporter neural stem cells were transplanted IA or intravenous at 24 hours after brain ischemia. In vivo BLI was used to track transplanted cells up to 2 weeks after transplantation and ex vivo BLI was used to determine single organ biodistribution.

Results—Immediately after transplantation, BLI signal from the brain was 12 times higher in IA versus intravenous injected animals ($P<0.0001$). After IA injection, 69% of the total luciferase activity arose from the brain early after transplantation and 93% at 1 week. After intravenous injection, 94% of the BLI signal was detected in the lungs ($P = 0.004$) followed by an overall 94% signal loss at 1 week, indicating lack of cell survival outside the brain. Ex vivo single organ analysis showed a significantly higher BLI signal in the brain than in the lungs, liver, and kidneys at 1 week ($P<0.0001$) and 2 weeks in IA ($P = 0.007$).

Correspondence to Raphael Guzman, MD, Department of Neurosurgery, Stanford University, School of Medicine and Lucile Packard Children's Hospital, 300 Pasteur Drive R211, Stanford, CA 94305-5327. raphaelg@stanford.edu.

Disclosures

None.

Conclusion—IA transplantation results in superior delivery and sustained presence of neural stem cells in the ischemic brain in comparison to intravenous infusion.

Keywords

biodistribution; bioluminescence imaging; cell transplantation; experimental; intra-arterial; ischemia; stem cells

Neural stem cell (NSC) transplantation represents a promising experimental therapeutic avenue for stroke.[1–3] Recent studies have demonstrated successful engraftment and functional recovery in animal models of cerebral ischemia,[4–10] and stem cell-based therapies are being evaluated for safety and efficacy in humans.[11,12] Minimally invasive intravascular delivery would carry several benefits over intraparenchymal transplantation.[13,14] Cells delivered in the vasculature gain superior access to injured tissue and an intravascular approach allows for a repeatable, multiple treatment paradigm. Additionally, the transplantation procedure carries significantly lower risks compared with stereotactic neurosurgery.

There are 2 methods of intravascular delivery: intravenous (IV) and intra-arterial (IA) transplantation. Intravascularly delivered cells can undergo directed chemotactic recruitment, transendothelial diapedesis, and subsequent intraparenchymal migration to the ischemic lesion.[4,5,15] IV infusion is an attractive candidate based on ease of administration and clinical precedent, but recent studies have reported poor cell delivery to the brain and suggested cell entrapment in peripheral organs.[16] IA delivery may overcome limitations of IV by using a more direct route to the central nervous system such as endovascular selective catheterization of intracerebral vessels for current stroke therapy.

A direct in vivo comparison of both intravascular cell delivery techniques with quantitative analysis of the cellular biodistribution is an important step toward further development of minimally invasive stem cell therapy for central nervous system diseases. We used an in vivo imaging approach to explore the biodistribution of transplanted NSCs in a mouse model of hypoxic–ischemia. We demonstrate a significant difference in delivery efficiency of NSCs to the ischemic brain between IA and IV transplantation.

Materials and Methods

Cell Culture

A murine multipotent NSC line derived from the external germinal layer of the mouse cerebellum (C17.2[17]) was used in these experiments. These NSCs have been shown to readily differentiate into noncerebellar neurons, astrocytes, and oligodendrocytes both in vitro and in vivo.[13,18] Cells were thawed at Passage 5 and thereafter cultured as previously described[4] in Dulbecco modified Eagle medium (Gibco, Grand Island, NY) supplemented with 10% fetal bovine serum (Gibco), 5% horse serum (Gibco), and 1% L-glutamine (2 mmol/L; Gibco) at 37°C and 5% CO_2.

Cell Transduction

Cells were transduced as previously described.[19] Briefly, a triple-fusion construct containing a firefly luciferase (Fluc), monomeric red fluorescent protein (RFP), and truncated version of sr39 thymidine kinase (FLuc-mRFP-tTK) was inserted into a lentiviral vector (Figure 1A). Viral particles were produced in 293T cells and NSCs were suspended with high-titer (>109 particles/mL) viral supernatants, centrifuged at 1800 g for 3 hours at 32°C, and incubated overnight at 37°C and 5% CO_2. One week after transduction, successfully transduced cells were isolated using RFP on a 3-laser fluorescence-activated cell sorter (Becton Dickinson, San Jose, Calif). The appropriate forward and side scatter and propidium iodide (10 μg/mL) gating was used to isolate viable cells. Cells isolated using fluorescence-activated cell sorter were grown in standard culture conditions for 2 weeks before transplantation at Passage 9. For MRI tracking, the cells were labeled with super paramagnetic iron oxide (SPIO) particles (Feridex IV; Berlex Laboratories, Wayne, NJ) as described previously.[20]

Hypoxia–Ischemia Model

All animal procedures were approved by Stanford University Administrative Panel on Laboratory Animal Care. Brain ischemia was induced using a hypoxic–ischemia model.[21] Nude hairless mice (10 weeks old, Nu/Nu; Charles River, Wilmington, Mass) underwent left common carotid artery occlusion with an aneurysm clip before inducing hypoxia at 8% O_2 for 30 minutes at 37°C. After hypoxia, reperfusion was obtained by removal of the aneurysm clip. Sham animals underwent the same procedure except occlusion of the left common carotid artery and hypoxia.

Cell Transplantation

Twenty-four hours after brain ischemia, randomly assigned animals (n = 12 for each group) received tail vein injection or IA injection of NSCs harboring the reporter gene as well as SPIO particles. NSCs were dissociated into a single cell suspension with trypsin. Cell viability, as assessed using the trypan blue dye exclusion method, was >95% in all groups. IV injections of 5×10^5 cells in 200 μL saline were administered through the tail vein. For IA injections, the ipsilateral carotid artery was again exposed, the external carotid artery was ligated with 6-0 silk, the superior thyroid and pterygopalatine arteries were coagulated, and 5×10^5 NSCs in 5 μL saline were injected into the common carotid artery using a 10-μL Hamilton syringe with a 33-G custom-made microneedle. Sham animals received saline injections through the tail vein or carotid artery. No difference in morbidity or mortality was found between either intravascular experimental group.

In control animals, 5×10^5 parental NSCs or fluorescence-activated cell sorter isolated reporter NSCs were stereotactically transplanted into the striatum or subcutaneously in the shoulder area. To correlate photon flux with cell number, serial dilutions (350′000 to 50′000, n = 3 per dilution) of reporter NSCs were transplanted to the striatum.

Bioluminescent Imaging

Bioluminescent imaging (BLI) was conducted on the IVIS Spectrum system (Xenogen Corporation, Alameda, Calif). Mice were given an intraperitoneal injection of 100 μL D-

luciferin (15 mg/mL in phosphate-buffered saline; Promega, Madison, Wis). Whole-body images were acquired for 1 minute. The BLI signal was recorded as maximum photon flux (photons/s/cm^2/sr). Living Image 3.0 software (Caliper Life Sciences, Hopkinton, Mass) was used to quantify maximum photon flux in regions of interest (ROIs) in the head and torso.

Magnetic Resonance Imaging

MRI was performed on a 7-T small animal scanner (Varian/GE Healthcare, Palo Alto, Calif). Ischemic lesions of all animals were visualized using a T2-weighted fast spin echo sequence (TR/TE 4000/62 ms; field of view = 3 cm; matrix = 256×256; slice thickness = 1 mm; number of excitations = 3) and the T2 hyperintense area quantified. High-resolution MRI of transplanted SPIO-labeled NSCs was obtained from paraformaldehyde-fixed brains immersed in fomblin (Specialty Fluids Co, Valencia, Calif). Brains were placed in a custom-built solenoidal radiofrequency coil and imaged using a 3-dimensional FIESTA sequence[22] (TR/TE = 7.8/3.9 ms; resolution = 100 μm isotropic voxels; number of excitations = 1).

Ex Vivo Assay

To resolve BLI signal from single organs, additional experimental groups of IA and IV transplanted animals were euthanized at 1 and 2 weeks (n = 6, n = 3 each). As a control for background signal, organs of nontransplanted animals were used. Brain, lungs, livers, and kidneys were removed; homogenized in a glass tissue homogenizer; and suspended in 1 mL of phosphate-buffered saline in 6-well plates. D-Luciferin solution was added to the wells and BLI images acquired and photon counts quantified as described earlier.

Immunohistochemistry

At 24 hours and 2 weeks after IV or IA transplant, subgroups of animals were transcardially perfused with 4% paraformaldehyde, brains were cut in 30-μm sections, and processed for immunohistochemistry. After blocking, sections were incubated overnight at 4°C with the following primary antibodies: anti-RFP (1:500) and anti-Fluc (1:500; Abcam, Cambridge, Calif). Vessels were stained using lectin (1:350; Vector Labs, Burlingame, Calif). Secondary antibodies were added for 4 hours at room temperature followed by nuclear stain with 4′,6-diamidino-2-phenylindole (1:5000; AnaSpec, San Jose, Calif). Sections were visualized on a laser scanning confocal microscope (LSM510; Zeiss). Cells were counted at 24 hours and 2 weeks after cell injection of IV and IA injected animals. Cells were counted in 3 animals per condition in 5 random ROIs per section in the ischemic and contralateral hemisphere. Three consecutive sections each spaced by 120 μm and centered at the level of the striatum were selected. Data are expressed as mean cell number/mm^2.

Statistical Analysis

Quantitative data were expressed as mean ± SEM. Means were compared using 1-way analysis of variance and Student *t* test. The Bonferroni method of correction was used. $P<0.05$ was considered statistically significant.

Results

Construction and Validation of the Reporter Cell Line

The flow cytometry plot illustrates the subset of RFP-positive NSCs selected as the transduced population (Figure 1B). Both the grossly transduced population (Tube B) and the RFP-positive sorted subpopulation (Tube A) of NSCs exhibited luciferase activity in vitro in contrast to the wild-type parental cell line (Tube C; Figure 1B inset). Only sorted cells were used for biodistribution experiments. To confirm reporter gene activity and specificity of BLI, sorted RFP-positive NSCs were transplanted subcutaneously into the shoulder (Figure 2A, arrowhead) and stereotactically into the striatum (Figure 2B, arrowhead) contralateral to parental nontransduced cells (Figure 2A–B, arrows). BLI demonstrated luciferase activity of sorted NSCs above the background. Parental NSCs without the triple-fusion reporter gene on the contralateral side did not exhibit any luciferase activity above the background. An in vivo cell dilution curve was obtained allowing the correlation of photon flux to cell numbers (Figure 1C).

MRI confirmed infarction by the presence of a hyperintense corticostriatal lesion on T2-weighted images (Figure 2C). The mean infarct volume was 49 mm^3 ± 9 (SD) and there was no statistically significant difference between the IV and IA transplanted groups.

In Vivo Assessment of Biodistribution

Immediately after transplantation of 5×10^5 RFP-positive NSCs, BLI demonstrated a marked difference in biodistribution of NSCs between IA and IV delivery. After IA injections, all animals showed a significant amount of luciferase activity in the head (Figure 3A). In contrast, IV infused animals had predominant torso-distributed luciferase activity, suggesting the presence of cells in the lungs (Figure 3C). At 1 week after cell transplant, BLI indicated only a slight reduction in signal from the head in IA animals (Figures 3B and 4B). In IV injected mice, however, there was almost a total reduction in luciferase activity from the lungs (Figures 3D and 4B). Intravascular transplantation into sham-lesioned animals did not demonstrate any photon flux above the background in the head ROIs.

To corroborate the BLI findings, high-resolution iron-sensitive FIESTA MRI also demonstrated the presence of transplanted SPIO-labeled NSCs in the ischemic brain. Reformat FIESTA images in 3 planes (Figure 3G–I) demonstrate a cell distribution comparable to the aggregate bioluminescence imaging results (Figure 3A–B).

Quantification of Luciferase Activity

Quantification of photon counts in ROIs encompassing the head and the torso of each experimental animal were drawn to determine the biodistribution of transplanted cells after IA and IV delivery (Figure 4). We found significantly higher photon counts from head ROIs in the IA groups as compared with the IV group immediately (Figure 4A, $P<0.001$) and 1 week after transplantation (Figure 4B, $P = 0.025$). Conversely, IV transplanted animals demonstrated a significantly higher signal in the torso than IA injected animals immediately (Figure 4A, $P = 0.014$) and 1 week after transplantation (Figure 4B, $P<0.001$). The temporal profile analysis showed that over 7 days, there is a 32% signal loss in the brain in IA injected

animals versus a 91% signal loss in the torso of IV injected animals, indicating lack of survival outside of the brain (Figure 4C). In IV injected animals, the number of cells reaching the brain is very low and decreases by 94% over 7 days. The same holds true for the torso signal in IA injected animals in which a low initial cell signal decreases by 74% over 7 days (Figure 4C).

Assumptions on total cell numbers measured using in vivo BLI was made based on the cell dilution curve. An estimate number of 3.07×10^5 cells entered the brain after IA injection with a drop to 2.76×10^5 at 7 days. This would represent 61% and 55% of the injected cells, respectively.

In vivo imaging past 7 days did not demonstrate significant luciferase activity in transplanted animals, which may represent the detection limitation of the method in vivo. Thus, in an effort to further characterize the specific brain, lung, liver, and kidney biodistribution of transplanted NSCs, and to account for any experimental error occurring from different organ tissue depth and light scattering during BLI acquisition, animals were euthanized for whole organ luciferase assays. These ex vivo studies allowed for a more sensitive measure of the presence of transplanted cells in experimental animals. At 1 week, IA transplanted animals had 69% of the total observed signal from the brain versus 27% in IV transplanted animals (Figure 5A). In IA transplanted animals, the brain signal was significantly higher than the rest of the organs at 1 week (Figure 5A, $P<0.0001$) and 2 weeks (Figure 5B, $P = 0.007$). Comparison of the total photon flux in the brain between IA and IV showed the IA signal to be >3 times the one in IV at 1 week ($P = 0.0003$; Figure 5A) and more than double at 2 weeks ($P<0.0001$; Figure 5B). Background photon flux was measured at 52 357 (p/s/cm^2/sr), which was not significantly different from the lung and kidney signal in both IA and IV injected animals.

The presence of luciferase immunoreactive NSCs in the brain (box in 5C) was confirmed by immunohistochemistry at 24 hours (Figure 5D–E) and 2 weeks (Figure 5F). Cell counts in IA and IV injected animals at 24 hours in the ipsilateral and contralateral hemisphere corroborated the imaging findings. There were significantly more cells in the ipsilateral hemisphere in both the IA and IV group at 24 hours and 2 weeks ($P<0.05$). Significantly more cells were counted in the IA versus the IV injected animals (at 24 hours 12.1 ± 1.3 cells/mm^2 versus 0.1 ± 0.02 cells/mm^2, $P<0.01$; at 2 weeks 9.8 ± 0.9 cells/mm^2 versus 0.005 ± 0.02 cells/mm^2, $P<0.001$).

Discussion

Detailed knowledge about the biodistribution of transplanted NSCs after IV and IA injection is crucial to the development of intravascular stem cell therapy for stroke. Histological methods are often limited by incomplete analysis of anatomic distribution and therefore can harbor significant sampling error. These studies also cannot account for the dynamics of initial and secondary redistribution. We therefore created a BLI reporter NSC line allowing us to perform whole-body imaging with high sensitivity. BLI further allowed us to keep experimental animals alive and observe the initial engraftment and redistribution of transplanted NSCs at later time points.

Within the realm of experimental intravascular transplantation, IV infusion has been tested more than IA delivery.[13,14,23] However, recent studies have demonstrated unfavorable biodistribution after IV administration, finding significant numbers of transplanted cells in other organs than the brain and citing pulmonary passage as a major obstacle between transplanted cells and the injured brain.[16,24–28]

The present study demonstrates that IA delivery results in a significantly larger number of NSCs delivered to the ischemic brain when compared with the IV route. After IA injection, 69% of the total BLI signal was observed within the cerebrum versus 27% after IV. Using whole organ homogenates, we show that in IV transplanted animals, there is a significantly larger percentage of luciferase activity (and thus NSCs) in organs other than the brain as compared with the IA injected groups. Over time, there is a slight increase in the photon flux from the brain homogenates, suggesting secondary recruitment of NSCs from the periphery. The total photon flux observed in the ex vivo studies was almost 8 times less than in vivo, most likely due to the process of tissue homogenization and therefore the cell dilution curve (Figure 1C) is not applicable to the ex vivo study. The relative ratios of individual organs, however, were consistent with the head and torso findings in vivo.

Similar findings have been reported after IV infusion of mesenchymal stem cells with only approximately 2.5% of cells estimated to get past pulmonary passage.[29] In vivo imaging allowed us to study the dynamics of cell distribution over time. We found that 7 days after injection, 70% of the initial cell signal was still present in the brain. The observed photon flux correlated with approximately 2.76×10^5 cells. MRI of transplanted NSCs labeled with nanoparticles allowed spatial and tomographic information on biodistribution when coupled with BLI (Figure 3G–I). In contrast, after IV transplant, the absence of luciferase signal in the brain and torso (Figure 3D) suggests that NSCs do not redistribute to the damaged brain, but instead are cleared, probably by the innate immune system.[30] Several advantages of in vivo cellular imaging are demonstrated. In vivo molecular imaging not only allows a total body assessment of cell distribution after intravascular therapy, but also permits the study of cellular redistribution in the same animal over time. These findings are difficult to replicate with ex vivo methods. The cell count based on immunohistochemistry revealed findings consistent with in vivo imaging in terms of a predominant homing of cells to the injured hemisphere and a decrease of cell numbers over time. The histological cell count, however, does not represent a total cell number and might be flawed by sampling error. Therefore, direct correlation of the histological cell counts and in vivo or ex vivo BLI is not feasible.

Other studies have demonstrated functional benefit without cerebral engraftment, citing immunomodulation[31,32] and trophic support[33] as the primary mechanism of recovery. In previous studies, we demonstrated the influence of NSCs on the postischemic microenvironment, including synaptogenesis[34] and angiogenesis.[4] It could therefore be hypothesized that the unique presence of transplanted NSCs within the systemic circulation is sufficient for central nervous system repair. In addition, we have found a correlation between functional recovery and the number of transplanted NSCs detected in the brain,[4] indicating that both trophic support and engraftment may play an important role. We propose that engraftment can lead to sustained modulation of the microenvironment. Therefore, the

extended presence of NSCs in the brain after IA versus IV transplantation (Figure 4C) could be critical for the repair of damaged tissue.

Before translation into clinical paradigms, considerations about the human cerebral vasculature, human blood volume, and hemodynamics in addition to stem cell biological questions will need to be addressed. The human cerebral arterial network differs in a number of respects from the rodent. Although the same major arteries are involved in the formation of the circle of Willis, the complexity of the human brain leads to a more elaborate arterial and venous system, especially distal to the circle of Willis.

Conclusions

Our data support IA as a promising minimally invasive transplantation paradigm for stem cell-based therapies for brain ischemia. We found a higher efficiency of NSC delivery to the brain and an extended presence of transplanted cells in animals after IA versus IV delivery. The possibility of a selective endovascular catheter injection of NSCs to areas of damaged brain tissue and tissue at risk represents an attractive treatment modality. This approach would also allow for repeated treatments. Further studies will be needed to elucidate the ideal timing and cell dosage as well as the functional superiority of the IA injection technique.

Acknowledgments

We thank Evan Snyder, The Burnham Institute, for the donation of the C17.2 neural stem cell line and Elizabeth Hoyte for preparation of the illustrations.

Sources of Funding

This work was supported by the American Heart Association Grant AHA-0835274N and The Bechtel Foundation (to R.G.); Stanford University Bio-X Research Program (to X.G.); and the Swiss National Science Foundation Grants PBBEB-117034 and PASMP3-123221/1 and the Evelyn L. Neizer Fund (to R.H.A.).

References

1. Andres RH, Choi R, Steinberg GK, Guzman R. Potential of adult neural stem cells in stroke therapy. Regen Med. 2008; 3:893–905. [PubMed: 18947311]
2. Bliss T, Guzman R, Daadi M, Steinberg GK. Cell transplantation therapy for stroke. Stroke. 2007; 38:817–826. [PubMed: 17261746]
3. Bacigaluppi M, Pluchino S, Martino G, Kilic E, Hermann DM. Neural stem/precursor cells for the treatment of ischemic stroke. J Neurol Sci. 2008; 265:73–77. [PubMed: 17610905]
4. Guzman R, De Los Angeles A, Cheshier S, Choi R, Hoang S, Liauw J, Schaar B, Steinberg G. Intracarotid injection of fluorescence activated cell-sorted cd49d-positive neural stem cells improves targeted cell delivery and behavior after stroke in a mouse stroke model. Stroke. 2008; 39:1300–1306. [PubMed: 18309158]
5. Shen LH, Li Y, Chen J, Zhang J, Vanguri P, Borneman J, Chopp M. Intracarotid transplantation of bone marrow stromal cells increases axon-myelin remodeling after stroke. Neuroscience. 2006; 137:393–399. [PubMed: 16298076]
6. Kelly S, Bliss TM, Shah AK, Sun GH, Ma M, Foo WC, Masel J, Yenari MA, Weissman IL, Uchida N, Palmer T, Steinberg GK. Transplanted human fetal neural stem cells survive, migrate, and differentiate in ischemic rat cerebral cortex. Proc Natl Acad Sci U S A. 2004; 101:11839–11844. [PubMed: 15280535]

7. Honma T, Honmou O, Iihoshi S, Harada K, Houkin K, Hamada H, Kocsis JD. Intravenous infusion of immortalized human mesenchymal stem cells protects against injury in a cerebral ischemia model in adult rat. Exp Neurol. 2006; 199:56–66. [PubMed: 15967439]
8. Chen J, Li Y, Wang L, Zhang Z, Lu D, Lu M, Chopp M. Therapeutic benefit of intravenous administration of bone marrow stromal cells after cerebral ischemia in rats. Stroke. 2001; 32:1005–1011. [PubMed: 11283404]
9. Chen J, Sanberg PR, Li Y, Wang L, Lu M, Willing AE, Sanchez-Ramos J, Chopp M. Intravenous administration of human umbilical cord blood reduces behavioral deficits after stroke in rats. Stroke. 2001; 32:2682–2688. [PubMed: 11692034]
10. Chu K, Kim M, Park KI, Jeong SW, Park HK, Jung KH, Lee ST, Kang L, Lee K, Park DK, Kim SU, Roh JK. Human neural stem cells improve sensorimotor deficits in the adult rat brain with experimental focal ischemia. Brain Res. 2004; 1016:145–153. [PubMed: 15246850]
11. Kondziolka D, Steinberg GK, Cullen SB, McGrogan M. Evaluation of surgical techniques for neuronal cell transplantation used in patients with stroke. Cell Transplant. 2004; 13:749–754. [PubMed: 15690976]
12. Kondziolka D, Steinberg GK, Wechsler L, Meltzer CC, Elder E, Gebel J, Decesare S, Jovin T, Zafonte R, Lebowitz J, Flickinger JC, Tong D, Marks MP, Jamieson C, Luu D, Bell-Stephens T, Teraoka J. Neurotransplantation for patients with subcortical motor stroke: a phase 2 randomized trial. J Neurosurg. 2005; 103:38–45. [PubMed: 16121971]
13. Guzman R, Choi R, Gera A, De Los Angeles A, Andres RH, Steinberg GK. Intravascular cell replacement therapy for stroke. Neurosurg Focus. 2008; 24:E15. [PubMed: 18341391]
14. Hicks A, Jolkkonen J. Challenges and possibilities of intravascular cell therapy in stroke. Acta Neurobiol Exp (Wars). 2009; 69:1–11. [PubMed: 19325636]
15. Walczak P, Zhang J, Gilad AA, Kedziorek DA, Ruiz-Cabello J, Young RG, Pittenger MF, van Zijl PC, Huang J, Bulte JW. Dual-modality monitoring of targeted intraarterial delivery of mesenchymal stem cells after transient ischemia. Stroke. 2008; 39:1569–1574. [PubMed: 18323495]
16. Gao J, Dennis JE, Muzic RF, Lundberg M, Caplan AI. The dynamic in vivo distribution of bone marrow-derived mesenchymal stem cells after infusion. Cells Tissues Organs. 2001; 169:12–20. [PubMed: 11340257]
17. Ryder EF, Snyder EY, Cepko CL. Establishment and characterization of multipotent neural cell lines using retrovirus vector-mediated oncogene transfer. J Neurobiol. 1990; 21:356–375. [PubMed: 2307979]
18. Snyder EY, Deitcher DL, Walsh C, Arnold-Aldea S, Hartwieg EA, Cepko CL. Multipotent neural cell lines can engraft and participate in development of mouse cerebellum. Cell. 1992; 68:33–51. [PubMed: 1732063]
19. Ray P, Tsien R, Gambhir SS. Construction and validation of improved triple fusion reporter gene vectors for molecular imaging of living subjects. Cancer Res. 2007; 67:3085–3093. [PubMed: 17409415]
20. Guzman R, Bliss T, De Los Angeles A, Moseley M, Palmer T, Steinberg G. Neural progenitor cells transplanted into the uninjured brain undergo targeted migration after stroke onset. J Neurosci Res. 2008; 86:873–882. [PubMed: 17975825]
21. Ashwal S, Tone B, Tian HR, Chong S, Obenaus A. Comparison of two neonatal ischemic injury models using magnetic resonance imaging. Pediatr Res. 2007; 61:9–14. [PubMed: 17211133]
22. Heyn C, Ronald JA, Mackenzie LT, MacDonald IC, Chambers AF, Rutt BK, Foster PJ. In vivo magnetic resonance imaging of single cells in mouse brain with optical validation. Magn Reson Med. 2006; 55:23–29. [PubMed: 16342157]
23. Willing AE, Lixian J, Milliken M, Poulos S, Zigova T, Song S, Hart C, Sanchez-Ramos J, Sanberg PR. Intravenous versus intrastriatal cord blood administration in a rodent model of stroke. J Neurosci Res. 2003; 73:296–307. [PubMed: 12868063]
24. Aicher A, Brenner W, Zuhayra M, Badorff C, Massoudi S, Assmus B, Eckey T, Henze E, Zeiher AM, Dimmeler S. Assessment of the tissue distribution of transplanted human endothelial progenitor cells by radioactive labeling. Circulation. 2003; 107:2134–2139. [PubMed: 12695305]

25. Lappalainen RS, Narkilahti S, Huhtala T, Liimatainen T, Suuronen T, Narvanen A, Suuronen R, Hovatta O, Jolkkonen J. The SPECT imaging shows the accumulation of neural progenitor cells into internal organs after systemic administration in middle cerebral artery occlusion rats. Neurosci Lett. 2008; 440:246–250. [PubMed: 18572314]

26. Pluchino S, Quattrini A, Brambilla E, Gritti A, Salani G, Dina G, Galli R, Del Carro U, Amadio S, Bergami A, Furlan R, Comi G, Vescovi AL, Martino G. Injection of adult neurospheres induces recovery in a chronic model of multiple sclerosis. Nature. 2003; 422:688–694. [PubMed: 12700753]

27. Jin K, Sun Y, Xie L, Mao XO, Childs J, Peel A, Logvinova A, Banwait S, Greenberg DA. Comparison of ischemia-directed migration of neural precursor cells after intrastriatal, intraventricular, or intravenous transplantation in the rat. Neurobiol Dis. 2005; 18:366–374. [PubMed: 15686965]

28. Fischer UM, Harting MT, Jimenez F, Monzon-Posadas WO, Xue H, Savitz SI, Laine GA, Cox CS Jr. Pulmonary passage is a major obstacle for intravenous stem cell delivery: the pulmonary first-pass effect. Stem Cells Dev. 2009; 18:683–692. [PubMed: 19099374]

29. Harting MT, Jimenez F, Xue H, Fischer UM, Baumgartner J, Dash PK, Cox CS. Intravenous mesenchymal stem cell therapy for traumatic brain injury. J Neurosurg. 2009; 110:1189–1197. [PubMed: 19301973]

30. Grundy MA, Sentman CL. Immunodeficient mice have elevated numbers of nk cells in non-lymphoid tissues. Exp Cell Res. 2006; 312:3920–3926. [PubMed: 17005178]

31. Pluchino S, Zanotti L, Rossi B, Brambilla E, Ottoboni L, Salani G, Martinello M, Cattalini A, Bergami A, Furlan R, Comi G, Constantin G, Martino G. Neurosphere-derived multipotent precursors promote neuroprotection by an immunomodulatory mechanism. Nature. 2005; 436:266–271. [PubMed: 16015332]

32. Borlongan CV, Hadman M, Sanberg CD, Sanberg PR. Central nervous system entry of peripherally injected umbilical cord blood cells is not required for neuroprotection in stroke. Stroke. 2004; 35:2385–2389. [PubMed: 15345799]

33. Borlongan CV, Skinner SJ, Geaney M, Vasconcellos AV, Elliott RB, Emerich DF. Intracerebral transplantation of porcine choroid plexus provides structural and functional neuroprotection in a rodent model of stroke. Stroke. 2004; 35:2206–2210. [PubMed: 15284450]

34. Liauw J, Hoang S, Choi M, Eroglu C, Sun GH, Percy M, Wildman-Tobriner B, Bliss T, Guzman RG, Barres BA, Steinberg GK. Thrombospondins 1 and 2 are necessary for synaptic plasticity and functional recovery after stroke. J Cereb Blood Flow Metab. 2008; 28:1722–1732. [PubMed: 18594557]

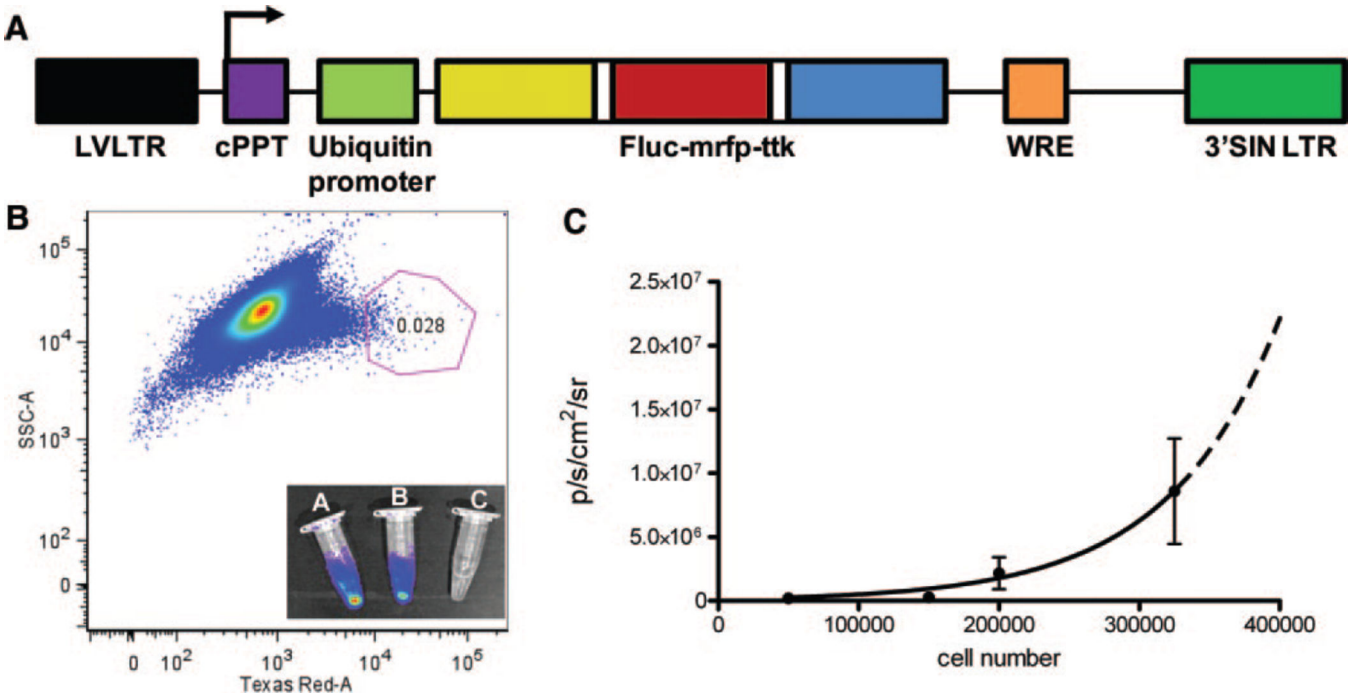

Figure 1.

Mouse NSCs were transduced with a triple-fusion reporter gene encoding a firefly luciferase (Fluc), monomeric red fluorescent protein (mrfp), and truncated thymidine kinase (ttk; A). Successfully transduced cells were isolated using fluorescent activated cell sorting for RFP expression (B). Sorted cells (Tube A) exhibited increased luciferase activity when compared with the unsorted population (Tube B) and wild-type parental NSCs (Tube C, inset B). An in vivo dilution curve of stereotactically transplanted cells into the brain was performed to correlate in vivo animal photon flux with numbers of transplanted cells (C).

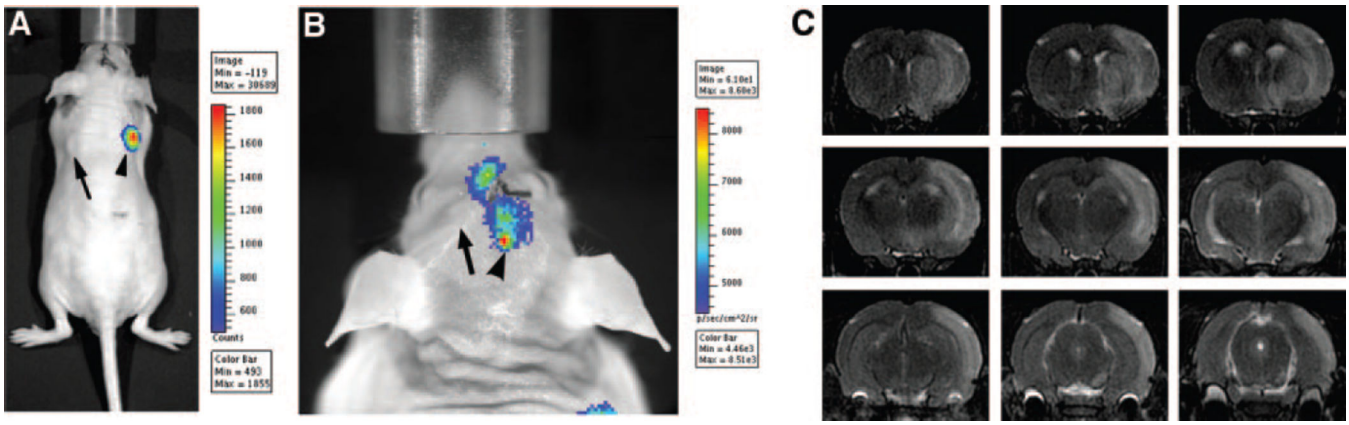

Figure 2.

NSCs were tested for specific luciferase activity in vivo before biodistribution studies. RFP-positive NSCs transplanted subcutaneously in the right shoulder and stereotactically into the right striatum (arrowhead in A–B) produced signal as observed by BLI, whereas wild-type parental NSCs transplanted on the contralateral side (arrow in A–B) did not. T2-weighted MRI was used to confirm the presence of hypoxic–ischemic stroke before transplant. A distinct hyperintense lesion was evident in the ipsilateral cortex and striatum 24 hours after stroke (C).

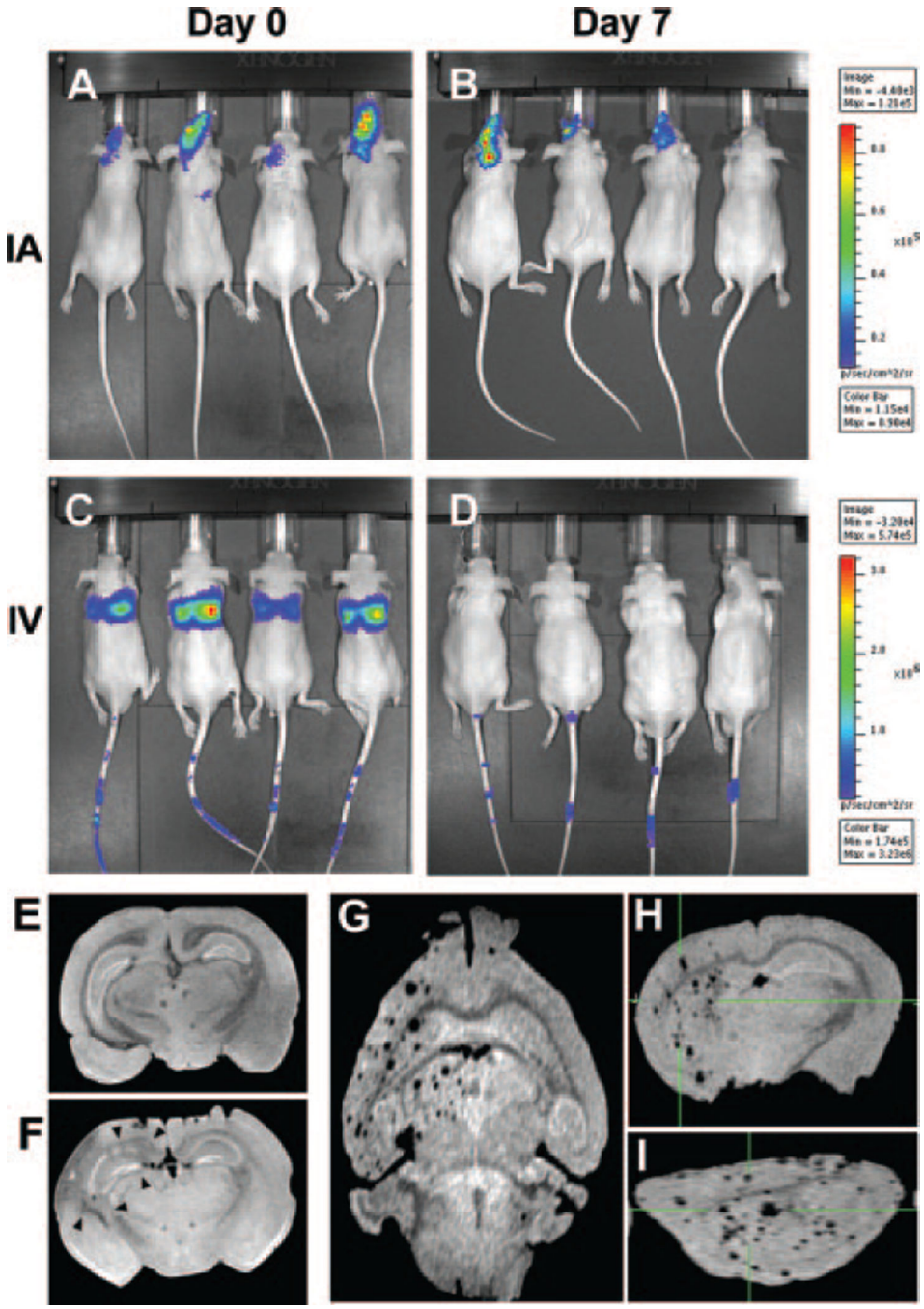

Figure 3.

Twenty-four hours after stroke, 5×10^5 NSCs were injected either in the ipsilateral internal carotid artery (IA) or the tail vein (IV). Immediately after IA transplant, a large amount of photon flux in the head of experimental animals was observed (A). In contrast, IV injection gave rise to large amounts of NSCs in the torso (C). One week after transplant, there was a decrease in signal in both groups; however, IA maintained more transplanted NSCs in the brain (B), whereas IV demonstrated a loss of signal (D). FIESTA MRI (E–G) was used to track transplanted NSCs labeled with SPIO nanoparticles. A normal coronal MRI at the

hippocampus level is shown in (E) and a brain after hypoxia–ischemia in (F) where the arrowheads delineate the stroked area. Transplanted SPIO-labeled NSCs produced a hypointense signal as seen in reformatted FIESTA images in an axial (G), coronal (H), and sagittal (I) view. A cell distribution in the ischemic hemisphere comparable to images obtained with BLI is seen (G).

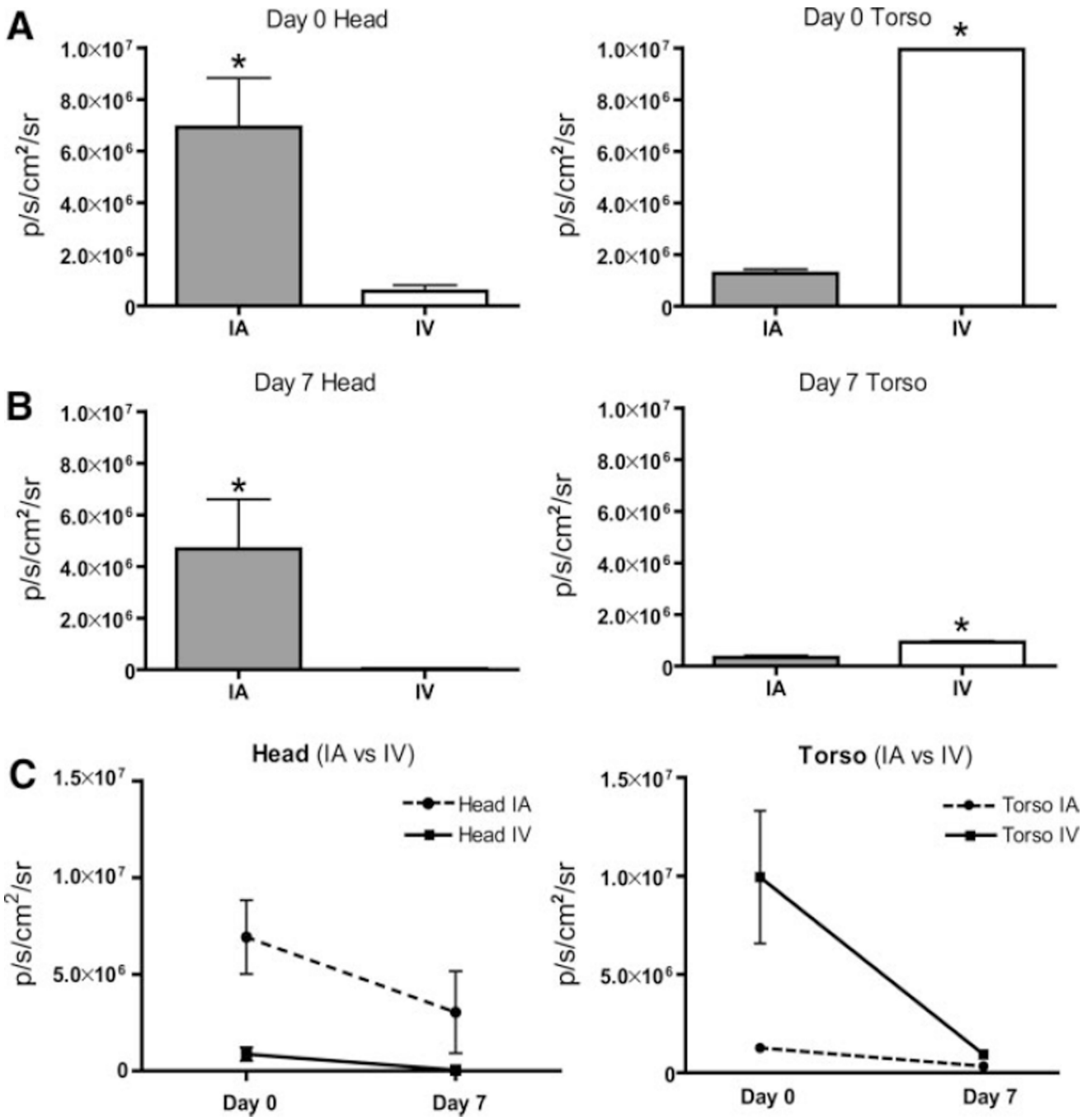

Figure 4.

A, Quantification of BLI findings measuring photon output in ROIs covering the brain and torso. More cell signal is measured in the brain immediately (A, *P<0.001, *P = 0.014) and at 7 days (B, *P = 0.025, *P<0.001) in IA as compared with IV injected animals. Plot illustrating the luciferase signal in each experimental group over time (C). One week after transplant, only the IA delivered group exhibits any significant luciferase signal in the head. (n = 12, data shown as mean ± SEM).

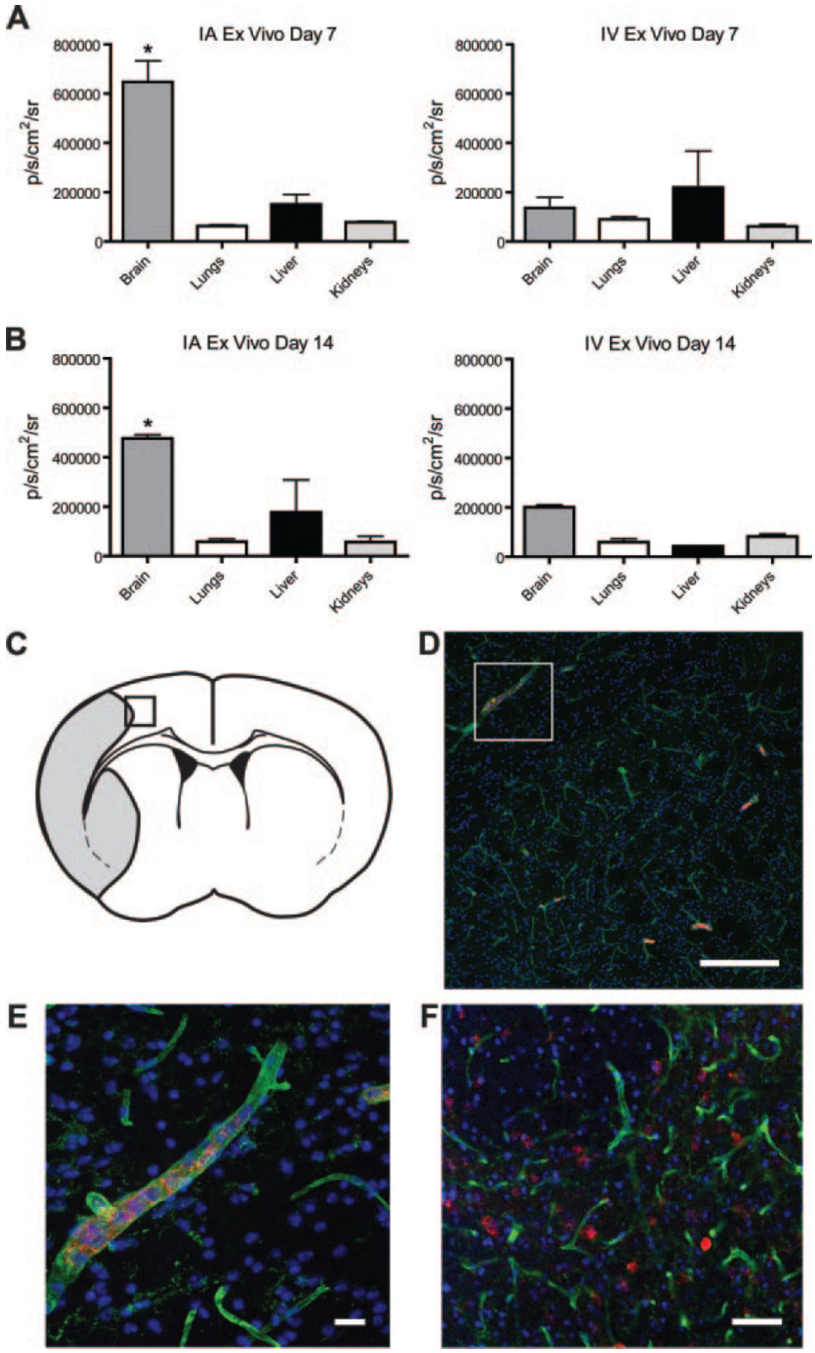

Figure 5.

To further explore the biodistribution without light absorption and scattering associated with in vivo BLI, ex vivo biodistribution was determined by whole organ homogenization for the brain, lungs, liver, and kidneys. In IA transplanted animals, the brain signal was significantly higher than the rest of the organs at 1 week (A, n = 6, **P*<0.0001) and 2 weeks (B, n = 3, **P* = 0.007). No significant difference was seen in IV transplanted animals (data shown as mean ± SEM). At 24 hours (D–E) and 2 weeks (F) after transplant, luciferase immunoreactive NSCs were observed in IA transplanted animals confirming the luciferase activity to be

arising from transplanted cells (box in C depicts area represented in D at 24 hours and F at 2 weeks). Higher magnification image at 24 hours after transplantation shows an intravascular (lectin; green) location of transplanted luciferase-positive NSCs (red; E, scale bar 10 μm), whereas an intraparenchymal migration is observed at 2 weeks (F). Nuclei are stained with DAPI (blue). Scale bars D = 200 μm, E = 20 μm, F = 50 μm.